

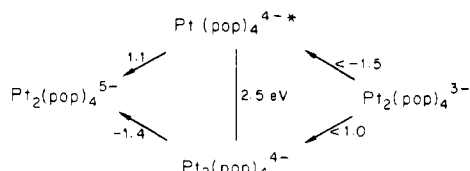
the hypothesis of electron-transfer quenching. Observation of separated redox products by flash photolysis would be unlikely in view of the Coulombic forces involved. A plot of $(RT/F) \ln k_{et}$ vs. amine $E_{1/2}$ values is shown in Figure 1.

A value of 1.1 ± 0.2 V for $E^\circ(\text{Pt}_2(\text{pop})_4^{4+/5-})$ is obtained by fitting the data in Table I to the equation

$$(RT/F) \ln k_{et} = ((RT/F) \ln \nu_{et}) - (\lambda(1 + \Delta G/\lambda)^2/4) \quad (1)$$

where $\Delta G = E^\circ(\text{NR}_3^{+/0}) - E^\circ(\text{Pt}_2(\text{pop})_4^{4+/5-}) + w_p - w_r$ (w_p and w_r are Coulombic work terms¹⁶) and ν_{et} is the frequency and λ the reorganization energy for electron transfer.²⁰ This value is larger than the corresponding values of 0.8 V for $\text{Ru}(\text{bpy})_3^{2+/+16}$ and ≈ 0.5 V for $\text{Rh}_2(\text{br})_4^{2+/+}$ ($\text{br} = 1,3\text{-diisocyanopropane}$).²¹ The reason for the lower k_q values for quenchers 2-4 reported here compared to those for $\text{Ru}(\text{bpy})_3^{2+/+16}$ is a result of the much larger value of λ for $\text{Pt}_2(\text{pop})_4^{4+/5-}$ (1.4 ± 0.2 V) compared to $\text{Ru}(\text{bpy})_3^{2+/+}$ (0.5 V).¹⁶ Since calculated values for the outer-sphere contribution to λ differ by less than 0.1 V, most of this difference can be ascribed to a larger inner-sphere reorganization energy for $\text{Pt}_2(\text{pop})_4^{4+/5-}$. This is to be expected given the differing natures of the excited-state distortions for $\text{Ru}(\text{bpy})_3^{2+/+22}$ and $\text{Pt}_2(\text{pop})_4^{4+/5-}$. This distortion is also expected to influence the $\text{Pt}_2(\text{pop})_4^{4+/5-}$ electron-transfer self-exchange rate. A maximum value of $2 \times 10^3 \text{ dm}^3 \text{ mol}^{-1} \text{ s}^{-1}$ is calculated for this rate constant using the data in Table I.²³

An energy level diagram summarizing the excited-state redox thermodynamics in terms of E° values (V vs. SCE) can now be constructed:



where E° for $\text{Pt}_2(\text{pop})_4^{3-/4-}$ is from ref 9 (H_2O), and the E° values for $\text{Pt}_2(\text{pop})_4^{4-/5-}$ and $\text{Pt}_2(\text{pop})_4^{3-/4-}$ are calculated from the excited-state reduction potentials and $E_{\text{O-O}} = 2.5 \text{ eV}$.^{5,8,9,24} Thus, in comparison to $\text{Ru}(\text{bpy})_3^{2+/+}$, $\text{Pt}_2(\text{pop})_4^{4+/5-}$ is thermodynamically both a better oxidant and reductant. This advantage is partly mitigated by the large excited-state distortion for $\text{Pt}_2(\text{pop})_4^{4+/5-}$, manifested in a large energy of reorganization.

Contrary to a previous report,¹ we have found $\text{Pt}_2(\text{pop})_4^{4-}$ to be stable in acid ($1.0 \text{ dm}^3 \text{ mol}^{-1} \text{ HClO}_4$), although decomposition to $\text{Pt}_2(\text{pop})_4\text{Cl}_2^{4-13,15}$ in $1.0 \text{ dm}^3 \text{ mol}^{-1} \text{ HCl}$ was observed. Thermal decomposition is rapid in basic media ($\text{pH} > 10$).

The quantum yield for the triplet phosphorescent state of $\text{Pt}_2(\text{pop})_4^{4-}$ is determined to be 0.52 ± 0.07 (deoxygenated H_2O ,

$25 \pm 3^\circ \text{C}$).²⁵ This, coupled with the measured lifetime of $6.2 \mu\text{s}$ (deoxygenated H_2O , 24°C),⁴ enables values of $8.4 \times 10^4 \text{ s}^{-1}$ for the radiative rate constant and $7.7 \times 10^4 \text{ s}^{-1}$ for the nonradiative rate constant to be calculated. The long lifetime and large quantum yield both contribute to efficient excited-state reactivity.

Acknowledgment. We thank Dr. George H. Allen of the University of North Carolina at Chapel Hill for the laser lifetime measurement and Professor Allen J. Bard and Dr. Joon Kim for providing us with preliminary electrochemical results. This work was supported by the donors of the Petroleum Research Fund, administered by the American Chemical Society, and by a Du Pont Corp. grant to Bowdoin College, Fund 65411-5026. A generous loan of K_2PtCl_4 by the Johnson-Matthey Company is also gratefully acknowledged.

Registry No. 1, 100-22-1; 2, 366-29-0; 3, 99-97-8; 4, 121-69-7; 5, 603-34-9; $\text{Pt}_2(\text{pop})_4^{4-}$, 80011-25-2.

(25) The quantum yield was determined relative to quinine sulfate in $1.0 \text{ dm}^3 \text{ mol}^{-1} \text{ H}_2\text{SO}_4$, for which $\Phi_{\text{em}} = 0.546$ (Demas, J. N.; Crosby, G. A. *J. Phys. Chem.* 1971, 75, 991-1024). Emission spectra obtained with a Perkin-Elmer Model 654-40 fluorescence spectrophotometer were corrected for instrument response and converted to wavenumbers prior to integration (Morris, J. V.; Mahaney, M. A.; Huber, J. R. *Ibid.* 1976, 80, 969-974). The value reported represents the average of four determinations.

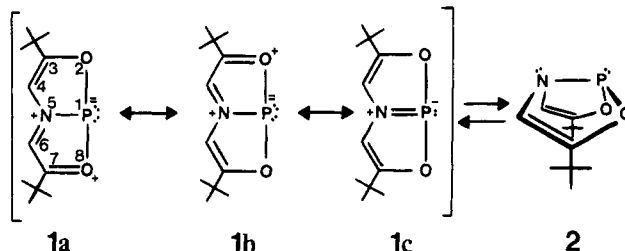
Synthesis and Structure of the First 10-P-3 Species

Scott Anthony Culley and Anthony J. Arduengo III*

Roger Adams Laboratory, Department of Chemistry
University of Illinois
Urbana, Illinois 61801

Received October 28, 1983

We report the synthesis and structure determination of the first 10-P-3 species, 5-aza-2,8-dioxo-3,7-di-*tert*-butyl-1-phosphabicyclo[3.3.0]octa-3,6-diene (ADPO).¹ The T-shaped phosphorus



ADPO

system of ADPO is the first member of a previously unknown class of compounds, a phosphorandiide.² ADPO can also be regarded as a phosphorus analog of the trithiapentalenes (10-S-3).

The synthesis of a compound that is free to choose between a 10- or 8-electron bonding scheme, without change in the ligation of the central atom, is of particular interest in the study of hypervalent bonding systems. For structures 1 and 2 the choice is clearly indicated by the geometry assumed by the molecule.

(1) The N-X-L system has been previously described (Perkins, C. W.; Martin, J. C.; Arduengo, A. J.; Lau, W.; Alegria, A.; and Kochi, J. K. *J. Am. Chem. Soc.* 1980, 102, 7753). In the present case the N-X-L identification is necessary to distinguish between the two possible structures for the ADPO system. Care must be taken to name the most important resonance structure that is free from multiple bonds at the center being described. It should also be noted that ClF_3 assumes the same T-shaped geometry of 1 and contains the 10-Cl-3 bonding system.

(2) The name phosphorandiide is suggested by the nomenclature previously used by Granth and Martin: Granth, I.; Martin, J. C. *J. Am. Chem. Soc.* 1978, 100, 7434.

(20) See eq 9, ref 16. Although in principle values of ν_{et} , λ , and ΔG can all be obtained from the data, the values for quenchers 1 and 5 were not used owing to large uncertainties in k_{et} for quencher 1 ($k_q \approx k_d$) and $E_{1/2}$ for quencher 5 (see Table I). Therefore, it was necessary to estimate ν_{et} as $10^{11}\text{--}10^{12} \text{ s}^{-1}$. Values of $w_p = -0.12 \text{ V}$ and $w_r = 0.00 \text{ V}$ were used to calculate $E^\circ(\text{Pt}_2(\text{pop})_4^{4+/5-})$ from ΔG .¹⁶

(21) Milder, S. J.; Goldbeck, R. A.; Kliger, D. S.; Gray, H. B. *J. Am. Chem. Soc.* 1980, 102, 6761-6764.

(22) Sutin, N.; Creutz, C. *Pure Appl. Chem.* 1980, 52, 2717-2738.

(23) This value was calculated by using the Marcus cross-relation (Cannon, R. D. "Electron Transfer Reactions"; Butterworths: London, 1980; pp 205-210) and a value of $1.0 \times 10^9 \text{ dm}^3 \text{ mol}^{-1} \text{ s}^{-1}$ for the amine self-exchange (Kowert, B. A.; Marcoux, L.; Bard, A. J. *J. Am. Chem. Soc.* 1972, 94, 5538-5550. Sorensen, S. P.; Bruning, W. H. *Ibid.* 1973, 95, 2445-2451). The cross-reaction rate constant for $\Delta G = 0$ was calculated by using $\nu_{et} = 10^{11} \text{ s}^{-1}$ and the smallest value of λ that reasonably fit the data (eq 1) in Table I, 1.2 V. The value of $2 \times 10^3 \text{ dm}^3 \text{ mol}^{-1} \text{ s}^{-1}$ is for $\mu = \infty$ and is decreased at finite ionic strengths. For instance, a value of $3 \text{ dm}^3 \text{ mol}^{-1} \text{ s}^{-1}$ is calculated for $\mu = 1.0 \text{ dm}^3 \text{ mol}^{-1}$ using the Debye-Hückel correction for ionic strength effects.

(24) Balzani, V.; Bolletta, F.; Gandolfi, M. T.; Maestri, M. *Topics Curr. Chem.* 1978, 75, 1-64. Entropy contributions are assumed to be less than 0.1 eV.^{5,16} Cyclic voltammetric measurements of the $\text{Pt}_2(\text{pop})_4^{4-}$ reduction in acetonitrile indicate that it occurs at much more negative potentials than the value of -1.4 V estimated here (Bard, A. J.; Kim, J., personal communication). Since a reversible potential has not been observed, no firm conclusions can be reached.

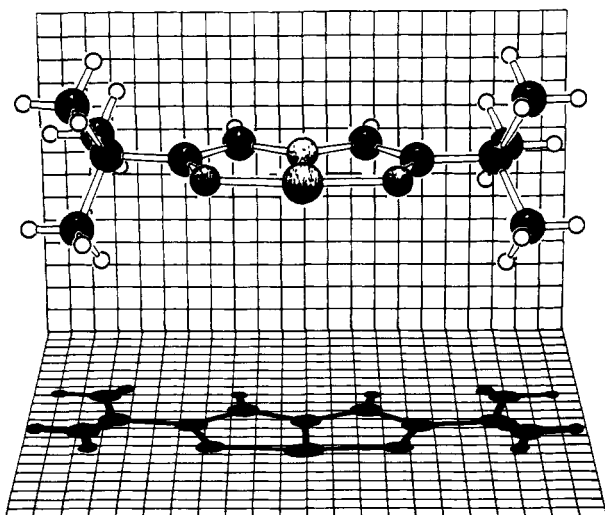


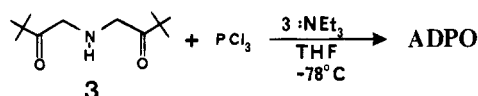
Figure 1. KANVAS⁴ drawing of 10-P-3 ADPO.

Table I. Bond Lengths and Angles in 10-P-3 ADPO

bond lengths, pm		bond angles, deg	
P-O	184.3 (10), 180.5 (10)	O-P-O	168.8 (4)
P-N	168 (1)	N-P-O	84.0 (5), 84.9 (5)
C-O	134 (2), 132 (2)	C-O-P	114.0 (9), 112.8 (9)
C-C _{ring}	135 (2), 132 (2)	C-N-P	118.2 (9), 117.3 (9)
C-N	139 (2), 138 (2)	C-C-N	111 (1), 110 (1)
		C-C-O	112 (1), 115 (1)

Structure 2 (8-P-3 ADPO) would be indicative of a preference for the 8-P-3 bonding scheme while the T-shaped geometry of 1 (10-P-3 ADPO) indicates the 10-P-3 bonding scheme. In this way the tendency of an atom to accept a hypervalent bonding scheme is freed from many of the complications due to a changing number of ligands.

ADPO is prepared by the reaction of the secondary amine 3 with PCl_3 in THF at -78°C .



ADPO exhibits a ^{31}P NMR resonance at +187 ppm in CD_2Cl_2 downfield of 85% phosphoric acid. The proton NMR (CD_2Cl_2) shows two resonances at δ 1.33 (s, 9 H) and 7.35 (d, $J_{\text{PH}} = 9$ Hz, 1 H). The proton-decoupled ^{13}C NMR of ADPO exhibits resonances at δ 28.0 (CH_3), 111.1 (d, $J_{\text{PC}} = 4.8$ Hz, C-4), and 169.9 (C-3). ADPO gives a molecular ion in the EI mass spectrum (70 eV) at $m/z = 241$, and after purification by sublimation or recrystallization from hexane/benzene satisfactory analyses (CHNP) were obtained. ADPO is thermally stable with a melting point of $138\text{--}140^\circ\text{C}$ but is sensitive to both water and oxygen.

A crystal of ADPO was obtained by sublimation and sealed in a glass capillary for X-ray crystallographic structure determination.³ Figure 1 illustrates the solid-state geometry observed for ADPO. The molecule is distinctly planar with no ring atom deviating from the best plane by more than 3 pm. The structure is clearly that of 10-P-3 ADPO.

Selected bond lengths and angles in 10-P-3 ADPO are given in Table I. The bond lengths and angles are similar to diox-

thiapentalenes⁵ and indicative of the 10-electron bonding system about phosphorus. While the hypervalent bonding scheme in 10-P-3 ADPO is not evident from the ^{31}P NMR spectrum,⁶ it is suggested by the downfield shift of the ring proton (δ 7.35). The chemical shift of the ring proton may be the result of positive charge delocalization in the π system as suggested by resonance structures 1a or 1b and ring current from the 10π -electron system. The latter is probably not of great importance since the P-O and P-N bond are long.⁷ The long P-N bond also suggests that 1c is not an important resonance contributor to the structure.

The ^{13}C NMR resonances in 10-P-3 ADPO are similar to those observed for a simple dioxathiapentalene,⁵ and as with the dioxathiapentalenes the equatorial-axial linkage of the two five-membered rings⁸ probably supplements the stability of 10-P-3 ADPO.

It is instructive to envision the formation of 10-P-3 ADPO by the addition of a nucleophile to an 8-P-2 center to give the 10-P-3 system.⁹ In this manner the addition of an oxygen (4) or nitrogen (5) lone pair must occur at phosphorus forcing the phosphide center to behave as an electrophile—indeed the stability of the 10-electron bonding system at phosphorus would need to be considerable.

The electron reorganization and deformation of the as yet unknown 8-P-3 ADPO (2) to 10-P-3 ADPO also provides insight into the structure of 10-P-3 ADPO. This electromorphic¹⁰ isomerization illustrates the ability of the electron-rich π -system ($\text{OC}=\text{CNC}=\text{CO}$) to donate two electrons into the σ -system about phosphorus and thus bring about valence-shell expansion. This view of the structure, which is also suggested by resonance structures 1a and 1b, is consistent with the structural and spectral data so far obtained on 10-P-3 ADPO. Further studies are in progress to characterize the bonding for this highly unusual system and extend this chemistry to other main-group elements. With appropriate substitution it is hoped that analogues of ADPO can be synthesized in which both 10-P-3 and 8-P-3 electromorphs can be observed.

Acknowledgment is made to the National Science Foundation (NSF CHE 81-04980) for its support of this work. This work was also supported in part by the University of Illinois NSF Regional Instrumentation Facility (NSF CHE 79-16100). We are grateful to Dr. Scott R. Wilson for the X-ray structure of 10-P-3 ADPO and Dr. J. C. Martin for helpful discussions.

Supplementary Material Available: A complete description of the X-ray crystallographic structure determination of 10-P-3 ADPO and tables of positional and thermal parameters (6 pages). Ordering information is given on any current masthead page.

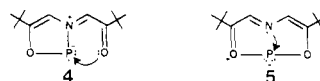
(5) Jacobsen, J. P.; Hansen, J.; Pedersen, C. T.; Pedersen, T. *J. Chem. Soc., Perkin Trans. 2* **1979**, 1521.

(6) The ^{31}P NMR shifts for the series 10-P-5 \rightarrow 10-P-4 \rightarrow 10-P-3 seems to move steadily downfield suggesting the importance of charge and the coordination number; see: Granoth, I.; Martin, J. C. *J. Am. Chem. Soc.* **1979**, *101*, 4623.

(7) See: Holmes, R. R. *ACS Monogr.* **1980**, No. 175. For representative bond lengths in 10-P-5 systems.

(8) Martin, J. C.; Perozzi, E. F. *J. Am. Chem. Soc.* **1974**, *96*, 3155.

(9) This approach to hypervalent bonding schemes has been recognized in the phosphorane systems.⁶ The two 8-P-2 systems under consideration here are



It should be noted that there is no evidence from low-temperature ^1H NMR spectra (-90°C , 360 MHz) for an asymmetric structure like 4, and the thermal ellipsoids of the oxygens in the X-ray structure 10-P-3 ADPO show no unusual distortion in this direction.

(10) We use the term electromorph to describe the relation between structures like 1 and 2 where a change in electron orbital occupancy and geometry is necessary to interconvert two isomers with the same connectivities. We presume that a structure like 2 can exist as an energy minimum as predicted by extended Hückel calculations. The energies calculated for 1 and 2 by extended Hückel are close and separated by a fairly small barrier. This interconversion is also orbital symmetry allowed.

(3) The crystal data were as follows: $\text{C}_{12}\text{H}_{20}\text{NO}_2\text{P}$, orthorhombic, space group $Pca2_1$, $a = 1149.3$ (4) pm, $b = 1155.8$ (3) pm, $c = 1115.4$ (4) pm, $Z = 4$, $D_c = 1.081$ g/cm³, crystal size $0.10 \times 0.22 \times 0.30$ mm. With 526 reflections of intensity greater than 2.58σ , the structure was solved by direct methods (MULTAN 80) and standard difference Fourier techniques. The final R factors were $R = 0.068$ and $R_w = 0.076$.

(4) The KANVAS program is based on the program, SCHAKAL, of E. Keller (Kristallographisches Institut der Universität Freiburg, FGR), which was modified by A. J. Arduengo, III (University of Illinois, Urbana, IL) to produce the back and shadowed planes. The planes bear a 50-pm grid, and the lighting source is at infinity.